*34th EPS Conference on Plasma Phys. Warsaw, 2 - 6 July 2007 ECA Vol.**31F**, P-4.142 (2007)*

Flow shearing and momentum balance in stellarators and rippled tokamaks

D. A. Spong[*], J. H. Harris[*], A. S. Ware[+], S. P. Hirshman[*], L. A. Berry[*]
[*]*Oak Ridge National Laboratory, Oak Ridge, Tennessee 37831 U.S.A.*
[+]*University of Montana-Missoula, Missoula, Montana 59812 U.S.A.*

Abstract

The structure of plasma flows in stellarators is of interest due their possible role in turbulence suppression, impurity transport, bootstrap current, and magnetic field error suppression. The PENTA code[1,2] has been developed to provide a self-consistent framework for evaluating radial fluxes of particle/energy, bootstrap current and plasma flows in 3D systems. Also, such a model has applications to the study of flow damping and bootstrap current levels in tokamaks with imperfect symmetry.

Introduction

From the neoclassical viewpoint, similar momentum balance mechanisms apply in three-dimensional systems as for perfectly symmetrical systems: i.e., diamagnetic and $E \times B$ flows are re-directed to parallel flows through viscous stress tensor effects, an equilibrium parallel flow is established through a balance between frictional and viscous forces (arising from inter-species collisions and trapped/passing friction), and Pfirsch-Schülter flows are generated to preserve overall incompressibility.[3] However, at a more detailed level, the small symmetry breaking (present even in quasi-symmetric systems) removes the degeneracy in the viscosities (present in symmetric systems); leads to nonlinear dependencies of the viscosities and stress tensor components on the electric field; and allows multiple, bifurcated electric field solutions. These differences can lead to plasma flows with strong directional variations and shearing rates within flux surfaces as well as the more conventional velocity shearing across flux surfaces. This raises a question as to whether the usual views of turbulence reduction, based on sheared $E \times B$ flows are applicable to situations where these other forms of velocity shearing are present. In order to address this issue, we have analyzed velocity shearing effects for a range of stellarators and rippled tokamaks using a recently developed moments method calculation for three-dimensional systems.

LHD SDC Regime plasma flows

A recent experimental achievement of substantial interest has been the generation of super dense core (SDC) plasmas in the LHD device with low recycling and high density gradient internal transport barriers.[4] This regime has been accessed via pellet injection and potentially offers an extrapolation to novel high density/low temperature ignition scenarios. In order to

understand the role of neoclassical flows in this regime, a sequence of model density profiles[5] has been assumed as shown in Fig. 3. These profiles become increasingly centrally peaked with a maximum density of 4.5×10^{20} m^{-3}; the associated temperature profiles are less peaked and pass through a range of central electron temperatures of $T_e(0) = 0.45$ (profile 1) to 0.85 keV (profile 6) with $T_i = T_e$. Figure 4 shows the profiles predicted by the PENTA moments method code[5] for the poloidal flow velocity associated with the profiles of Fig. 3. As may be seen, these become increasingly peaked in going from profile 3 to profile 4. Also, the poloidal component is significantly larger than the toroidal component (not shown). This characteristic can be seen from the flow vector arrow plots given in Figure 5 for an inner flux surface (top figure) and an outer flux surface (bottom figure).

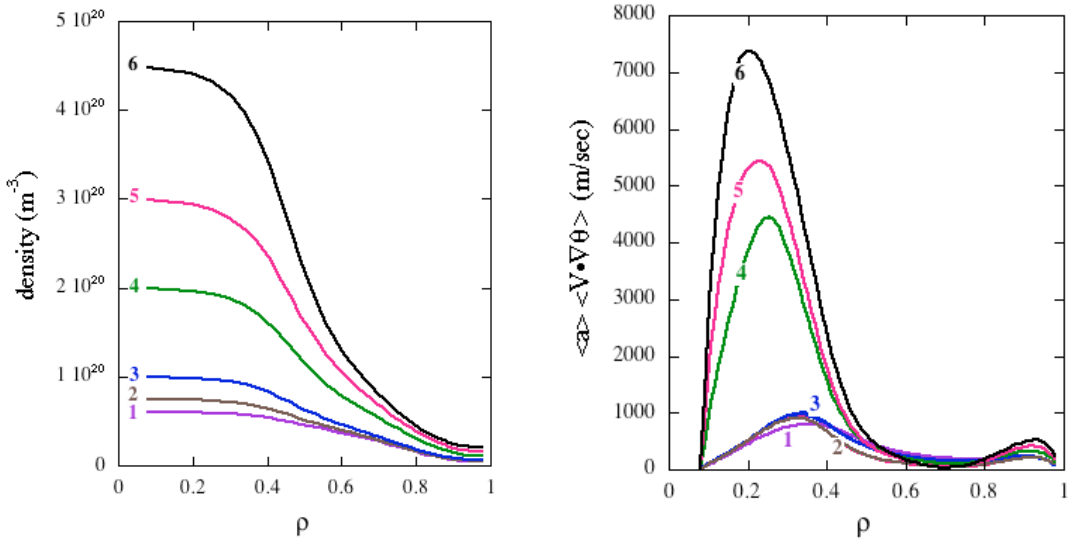

Figure 3 (left) – Model plasma density profiles used for moments method analysis of the LHD SDC regime, Figure 4 (right) – Predicted LHD poloidal flow velocity profiles obtained from the PENTA model.

The strong increase in poloidal flow velocity for the inner flux surfaces can be related to the variations of the neoclassical viscosity coefficients with the collisionality parameter $\nu_* = \nu R_0/\epsilon v_{th}$, electric field and radial location as the profiles evolve from profile 1 to 6. This variation is illustrated in Figure 6 where the viscosity coefficients (M_{1PP} which relates the poloidal component of the viscous stress tensor to the poloidal flow velocity) is plotted vs. the local collisionality at five different radial locations as the profiles evolve from profile 3 to 6. These collisionalities are in the lower end of the plateau regime ($\nu_* < 1$). While the collisionality and M_{1PP} viscous coefficient increase at all locations for this sequence of profiles, the viscosity near the central region increases more slowly than that in the outer half of the plasma.

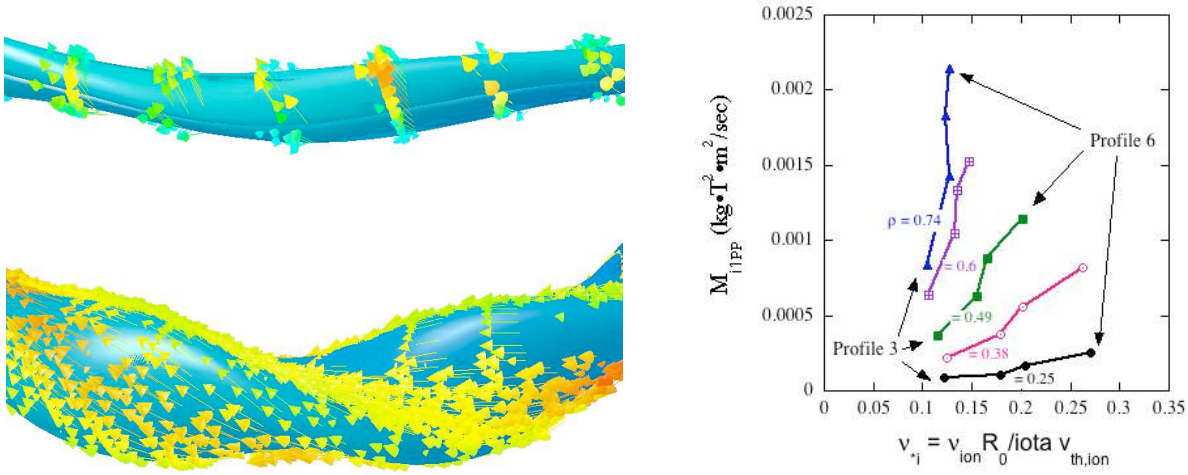

Figure 5 (left) – 3D arrow visualization of predicted flow velocities for inner (top) and outer (bottom) LHD flux surfaces, Figure 6 (right) – Trajectories of poloidal viscosity and collisionality for various radial locations as profiles evolve from profile 3 to 6 (see figure 3).

For profile 6, the viscosity at the innermost location ($\rho = 0.25$) is almost an order of magnitude lower than the viscosity at the outermost location ($\rho = 0.74$). The other components of the viscosity tensor have also been examined and show similar dependencies. This variation in the viscosity coefficient from inner to outer radii is caused by its variation in the three-dimensional parameter space of collisionality, electric field and flux surface location. The main source of the weaker variation near the magnetic axis can be related to the more shallow magnetic field variation there and a tendency for the constant |B| contours to become more poloidal with increasing β. This moves the peak in the viscosity vs. collisionality curve to somewhat higher collisionality and decreases the height of the peak relative to related curves for the outer flux surfaces. The high neoclassical velocity shearing region shown above is consistent with the experimentally observed transport barrier.

Plasma flows in rippled tokamaks

The edge regions of future tokamaks are increasingly three-dimensional due toroidal field ripple, ELM/RWM coils, and high permeability materials from welds and test blanket modules (ITER). Recently, coil models have been developed that allow calculation of free boundary rippled tokamak equilibria using the VMEC code. An example of such a calculation for ITER is shown in Fig. 7. The breaking of axi-symmetry removes the intrinsic ambipolarity expected in axi-symmetric tokamaks, and introduces the radial electric field as a new parameter that must be solved self-consistently. The PENTA code has recently been applied to a tokamak with ripple (a device with B = 2 T, R_0 = 2.5m, a = 0.88 m, 16 TF coils and q(0) = 1, q(1) = 3.3 has been chosen). The ambipolar electric field profile is shown in Fig. 8 for the

parameters: $n(0) = 10^{20}$ m^{-3}, $T_i(0) = T_e(0) = 600$ eV. Ion flow velocities are calculated, including the ripple-enhanced viscosities. As shown in Fig. 9, there are radial regions where poloidal flows can become large relative to other components. Fig. 10 shows the variation of the flows for a surface 50% out in flux. As can be seen, they are poloidally oriented on the outboard half of the torus, but more magnetic field aligned on the inboard side.

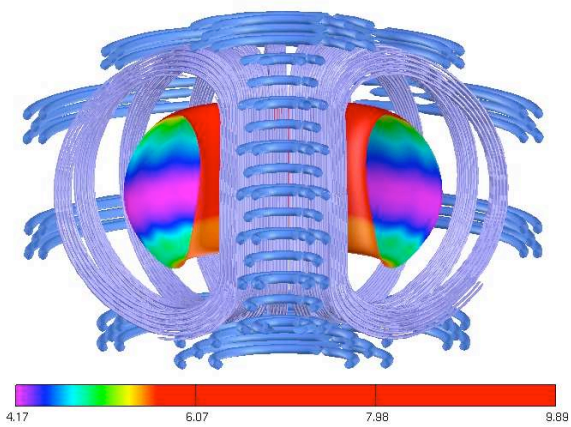

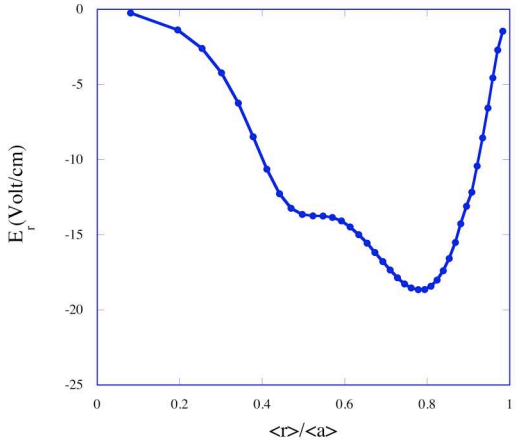

Figure 7 (left) – ITER equilibrium, showing rippled magnetic field strength, Figure 8 (right) – Ambipolar electric field profile for rippled tokamak.

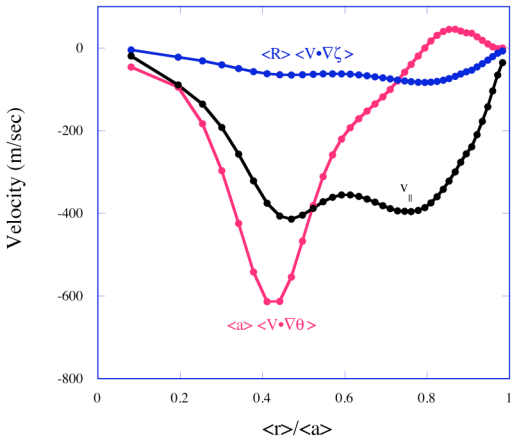

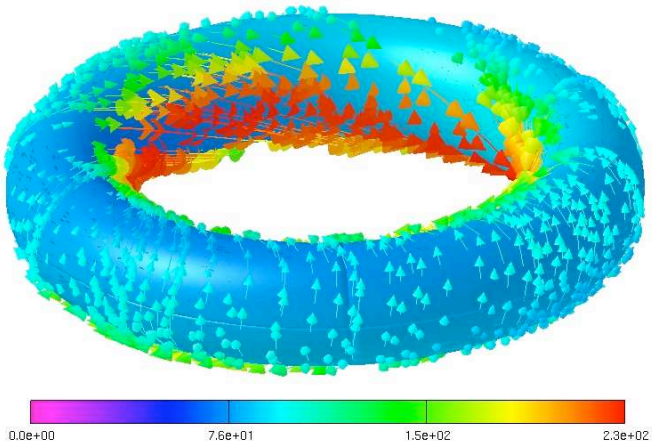

Figure 9 (left) – Ion flow velocity profiles for rippled tokamak, Figure 10 (right) – 3D arrow visualization of vector flow velocity field in rippled tokamak.

Acknowledgements – Research sponsored by the U.S. Department of Energy under Contract DE-AC05-00OR22725 with UT-Battelle, LLC.

[1] D. A. Spong, Phys. Plasmas **12** (2005) 056114.
[2] D. A. Spong, Fusion Sci. and Technol. **50** (2006) 343.
[3] H. Sugama, S. Nishimura, Phys. Plasmas **9** (2002) 4637.
[4] N. Ohyabu, et al., Phys. Rev. Lett. **97** (2006) 055002-1.
[5] D. A. Spong, J. H. Harris, A. S. Ware, S. P. Hirshman, L. A. Berry, Nuclear Fusion **47** (2007) 626.